Kinetics and Mechanism of the OH + HO_2 Reaction

James J. Schwab,* William H. Brune, and James G. Anderson

Department of Chemistry and Department of Earth and Planetary Sciences, Harvard University, Cambridge, Massachusetts 02138 *(Received: March 14, 1988)*

A discharge flow reactor with laser magnetic resonance and resonance fluorescence detection axes is used to measure the rate constant for the reaction of OH and HO_2 radicals by measuring the decay of OH in excess HO_2 under pseudo-first-order conditions. Particular care is taken to reduce impurity O and H atoms to low levels since their presence leads to an underestimate of the rate constant. The rate constant is measured to be $(8.0^{+3.0}_{-2.0}) \times 10^{-11}$ cm^3 molecule^{-1} s^{-1} at 298 K and 2 Torr after a small (3%) correction is made for the impurity atoms. It is argued that recent experimental and theoretical results indicate that the reaction mechanism is likely dominated by attack at the hydrogen end of HO_2 and that the reaction is unusually fast due a long-range attractive interaction.

Introduction

Perhaps no radical-radical reaction has commanded the fascination, patience, and attention to detail of kineticists more than the reaction of hydroxyl and hydroperoxyl radicals. Fred Kaufman many times referred to it as "the Holy Grail Reaction". Because Fred Kaufman has stood as an inspiration to the chemical kinetics and scientific communities, we feel it is a fitting tribute to present the results of our study of this reaction in this special issue. In the present study we have used a discharge flow reactor with laser magnetic resonance (LMR) and resonance fluorescence (RF) detection of reactants and reactive impurities. This system allowed very sensitive direct and simultaneous detection of OH, HO_2, O, and H and is ideal for this type of reaction. Great care has been taken to reduce the reactive impurity atoms O and H to very low levels, and a small correction has been applied to the data for those atoms which remained present.

The title reaction

$$OH + OH_2 \rightarrow H_2O + O_2 \qquad (1)$$

is interesting and important for a number of reasons. To the atmospheric and combustion chemist it is a dominant chain termination for HO_x radicals. To the theorist and theoretically inclined, reaction 1 is interesting for its possible pressure dependence, negative temperature dependence, and large rate constant.[1-5] To the laboratory kineticist, reaction 1 presents a great array of experimental challenges to be overcome in order to measure an accurate rate constant. There is considerable debate over whether the reaction mechanism is direct or complex. Because of the negative temperature dependence and apparent pressure dependence, the mechanism has been thought to be an example of an additon-rearrangement type reaction in much of the recent literature.[1,6] However, evidence is mounting that the pressure dependence is small or zero[2] and that the mechanism is best described by an an attack at the H-atom end of the HO_2 by the OH radical.[7] The mechanism will be discussed in more detail in the conclusion section.

The importance of this reaction has stimulated much interest in its rate constant, but its measurement has proven very difficult, and until recently yielded widely disparate results. The published measurements to date fall into three broad categories: first, studies of reaction 1 near 1 atm pressure, which have indicated $k_1 = (1-2) \times 10^{-10}$ cm^3 molecule^{-1} s^{-1};[4,5,8-10] second, the early low-pressure studies which indicated $k_1 = (3-5) \times 10^{-11}$ cm^3 molecule^{-1} s^{-1};[11-13] and third, recent low-pressure studies which have measured k_1 at $(6-10) \times 10^{-11}$ cm^3 molecule^{-1} s^{-1}.[1-3]

Fred Kaufman's example in pursuit of this rate constant is worthy of recall in this context. The first published work out of the Kaufman group on this reaction involved fitting experimental data to a computer model to obtain a "probable value" for k_1.[12] The rate constant determined in this manner depended on a number of other rate constants, and as better measurements of several rate constants in the model were made available, it became clear that even a well-conceived indirect method of determining k_1 was unacceptable. In addition, due to the close linkage of many of the radical reactions of OH and HO_2, one could not in practice nail down the value of k_1 without knowing the rate constant for at least reactons 2-5. Thus the course was clear; and Sridharan,

$$O + OH \rightarrow H + O_2 \qquad (2)$$

$$O + HO_2 \rightarrow OH + O_2 \qquad (3)$$

$$H + HO_2 \rightarrow \text{products} \qquad (4)$$

$$OH + H_2O_2 \rightarrow HO_2 + H_2O \qquad (5)$$

Kaufman, and co-workers first measured k_5,[14] then k_1[1] followed by k_4,[15] and k_3.[16] Keyser followed a similar course, measuring first k_5,[17] then k_1,[2] followed by k_3[18] and k_4.[19] Their rate constant determinations, along with those of other groups, have greatly increased the confidence in our knowledge of these rate constants.

(1) (a) Kaufman, F. *J. Phys. Chem.* **1984**, *88*, 4909. (b) Sridharan, U. C.; Qiu, L. X.; Kaufman, F. *J. Phys. Chem.* **1981**, *85*, 3361. (c) Sridharan, U. C.; Qiu, L. X.; Kaufman, F. *J. Phys. Chem.* **1984**, *88*, 1281.
(2) (a) Keyser, L. F. *J. Phys. Chem.* **1981**, *85*, 3667. (b) Keyser, L. F. *J. Phys. Chem.* **1988**, *92*, 1193.
(3) Temps, F.; Wagner, H. G. *Ber. Bunsen-Ges. Phys. Chem.* **1982**, *86*, 119.
(4) Kurylo, M. J.; Klais, O.; Laufer, A. H. *J. Phys. Chem.* **1981**, *85*, 3674.
(5) (a) Demore, W. B.; Tschuikow-Roux, E. *J. Phys. Chem.* **1974**, *78*, 1447. (b) DeMore, W. B. *J. Phys. Chem.* **1979**, *83*, 1113. (c) DeMore, W. B. *J. Phys. Chem.* **1982**, *86*, 121.
(6) Mozurkewich, M. *J. Phys. Chem.* **1986**, *90*, 2216.
(7) Toohey, D. W.; Brune, W. H.; Anderson, J. G. *J. Phys. Chem.* **1987**, *91*, 1215.
(8) (a) Hochnadel, C. J.; Ghormley, J. A., Ogren, P. J. *J. Chem. Phys.* **1972**, *56*, 4426. (b) Hochnadel, C. J., Sworski, T. J., Ogren, P. J. *J. Phys. Chem.* **1980**, *84*, 3274.
(9) Lii, R. R., Gorse, R. A., Sauer, M. C. Jr., Gorgen, S. *J. Phys. Chem.* **1980**, *84*, 819.
(10) Burrows, J. P.; Cox, R. A., Derwent, R. G. *J. Photochem.* **1981**, *16*, 147.
(11) Hack, W., Preuss, A. G., Wagner, H. G. *Ber. Bunsen-Ges. Phys. Chem.* **1978**, *82*, 1167.
(12) Chang, J. S.; Kaufman, F. *J. Phys. Chem.* **1978**, *82*, 1683.
(13) Burrows, J. P., Cliff, D. I., Harris, G. W., Thrush, B. A., Wilkinson, J. P. T. *Poc. R. Soc. London A* **1979**, *A368*, 463.
(14) Sridharan, U. C.; Reimann, B.; Kaufman, F. *J. Chem. Phys.* **1980**, *73*, 1286.
(15) Sridharan, U. C.; Qiu, L. X.; Kaufman, F. *J. Phys. Chem.* **1982**, *86*, 4569.
(16) Sridharan, U. C.; Klein, F. S.; Kaufman, F. *J. Chem. Phys.* **1985**, *82*, 592.
(17) Keyser, L. F. *J. Phys. Chem.* **1980**, *84*, 1659.
(18) Keyser, L. F. *J. Phys. Chem.* **1982**, *86*, 3439.
(19) Keyser, L. F. *J. Phys. Chem.* **1986**, *90*, 2994.

0022-3654/89/2093-1030$01.50/0

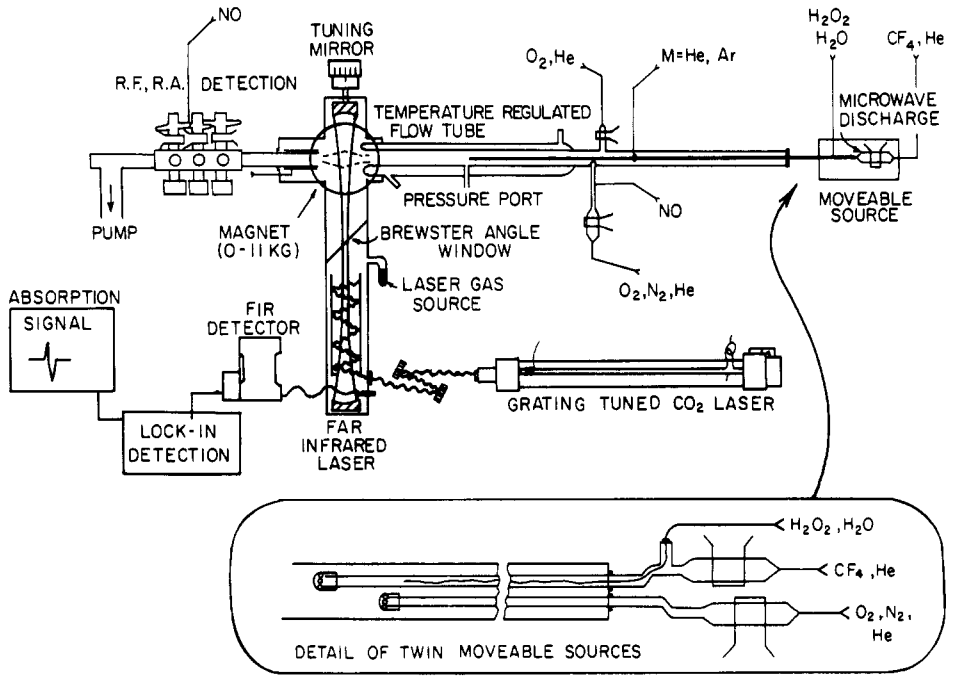

Figure 1. Schematic of the laser magnetic resonance–resonance fluorescence discharge flow apparatus used for these measurements. The inset shows the movable injectors used as radical sources.

It has also been the goal of this laboratory to study these HO_x reactions as a set in order to ensure self-consistency. Measurements of k_2 and k_3 were made prior to the present work[20] and there are plans for measurement of k_1 over extended temperature and pressure ranges. This paper reports the results of a room temperature determination of k_1 using a low-pressure discharge flow reactor with combined laser magnetic resonance and resonance fluorescence detecton of atoms and molecules.

Experimental Section

The apparatus has been described in detail previously[20] and is shown schematically in Figure 1. This section will review and describe the flow reactor and detection axes, the radical sources, and the experimental procedures used in these experiments.

Flow Reactor and Detection Axes. The main reaction zone of the flow apparatus consisted of a 70 cm long, 2.5 cm i.d. Pyrex tube located directly upstream of the laser magnetic resonance (LMR) axis. Decays of OH and concentrations of HO_2 were measured over this distance. A 20 cm long section of 2.5 cm i.d. Pyrex tube connected the LMR axis to the block containing the resonance fluorescence (RF) detection axes for O, H, and OH. As in previous work, the gaps at the LMR and RF axes could be effectively closed by inserting retractable glass tubing sections across them. All flow tube sections were coated with FEP Teflon to inhibit wall loss.

Laser magnetic resonance detection of both OH at 3.8 kG and HO_2 at 2.3 kG employed the σ-polarized 163-μm CH_3OH laser line pumped by 10R(38) CO_2 laser emission. The LMR spectrometer was calibrated for OH by using the $H + NO_2 \rightarrow OH + NO$ titration reaction. The calibration factor C_{OH}^{LMR} was measured at least twice a day and changed very little. This calibration factor was measured both with and without NO ([NO] = $(6 - 20) \times 10^{13}$ cm^{-3}) present, in order to correct for losses in the conversion of HO_2 to OH which occur mainly due to the reaction of OH with NO. The correction factor which accounted for these losses was 1.07 ± 0.02. Absolute concentrations of the HO_2 radical were determined by first converting the HO_2 to OH using excess NO. The OH signal from chemical conversion, S_{OH}^{NO}, the calibration factor, C_{OH}^{LMR}, and the correction factor yield the HO_2 concentration via

$$[HO_2] = 1.07(S_{OH}^{NO}/C_{OH}^{LMR}) \quad (6)$$

The ratio of the LMR sensitivities to OH and HO_2 was calculated as

$$R_C = 1.07(S_{OH}^{NO}/S_{HO_2}) \quad (7)$$

This ratio served as an indicator of the stability of the LMR spectrometer and as a convenient transfer calibration for obtaining average HO_2 concentrations. R_C ranged from 9.4 to 11.4, depending on laser and detection parameters.

The resonance fluorescence detection axes are descibed in detail in a previous paper.[20] A single axis was used for the detection of O and H atom impurities. The radiation source was a microwave discharge powered sealed lamp which excited emission at the 130.4-nm oxygen triplet and/or the 121.6-nm hydrogen Lyman α doublet. A CsI photomultiplier with a baffle-restricted field of view was set at a right angle to the lamp for detection. To isolate oxygen radiation a CaF_2 filter and a flowing N_2 cell was used; to isolate hydrogen radiation the CaF_2 filter was removed and a flowing O_2 cell filtered out the atomic oxygen radiation. The $N + NO \rightarrow O + N_2$ titration reaction was used to calibrate the axis for atomic oxygen; and $H + NO_2 \rightarrow OH + NO$ was used to calibrate the axis for atomic hydrogen. The signal to noise ratios at [O] or [H] = 10^9 cm^{-3} for 10-s integration periods was typically greater than 10 for O and about 4 for H. A second axis was used for resonance fluorescence detection of OH. A microwave discharge powered flowing lamp containing a trace of H_2O in helium excited radiation in the A–X band of OH; the resonantly scattered radiation was detected by a bialkali photomultiplier tube set at a right angle to the lamp and placed behind a band-pass filter, a lens, and a series of baffles. For detection of HO_2 by chemical conversion to OH, a Teflon-covered loop injector for addition of NO was placed 5 cm upstream of the detection axis. Calibration was carried out using the $H + NO_2$ titration; the signal to noise ratio at [OH] = 10^9 cm^{-3} for 10 second integration periods was typically about 2.

Hydrogen peroxide concentrations were measured by using absorption at 185 nm in a 10 cm long absorption cell prior to addition to the HO_2 source injector. The 90 wt % H_2O_2 was vacuum distilled to half or less of its original volume in order to reduce the amount of water vapor, which in turn reduces the amount of OH in the HO_2 source. The H_2O_2 purity was sufficiently high that the impurity [OH] in the HO_2 source was less than 5% of the [HO_2].

The pressure was measured with a Baratron Model 222 capacitance manometer calibrated against an oil manometer and

(20) Brune, W. H.; Schwab, J. J.; Anderson, J. G. *J. Phys. Chem.* **1983**, *87*, 4503.

the flows with Matheson Series 8142 flowmeters calibrated with a Brooks Vol-U-Meter piston gauge. Laboratory gases for these experiments were supplied by Matheson, with the following designations and stated purities: He (HP 99.995%) for bulk flow gas, He (UHP 99.999%) for flow through the discharges, CF_4 (99.7%), NO_2 (99.5%), NO (CP 99.0%), N_2 (UHP 99.9999%), and H_2 (Prepurified 99.95%). H_2O_2 (90 wt %) was vacuum distilled as described above; NO was purified as described previously.[20]

Radical Sources. The insert in Figure 1 shows the movable injectors used for the OH and HO_2 radical sources in these experiments. The radical injectors were 180 cm long, 6 mm o.d. glass tubes connected through a glass tee to an alumina discharge tube. The source reactions were initiated by a microwave discharge of a trace of CF_4 in helium to create a flow of F atoms. The OH or HO_2 radicals were made from the reactions of these F atoms with the H_2O or H_2O_2 added through the third arm of the glass tee via a long 1/16 in. o.d. Teflon line. The source reactions are then

$$F + H_2O \rightarrow OH + HF \quad (8)$$

$$F + H_2O_2 \rightarrow HO_2 + HF \quad (9)$$

By adjusting the concentrations and distances from the probe tip to the H_2O or H_2O_2 addition point, the HO_x-producing reactions were able to have a product of first-order rate times time of $kt \geq 8$ before the reactants entered the main flow. Both sources were tested for residual F atoms by setting the injector tips about 10 cm away from the atoms fluorescence axis and adding rougly 2×10^{14} cm^{-3} of H_2 to convert any unreacted F atoms to H atoms, and no change in H signal was observed. In the end, however, the H_2O for the OH source was added to the main flow rather than in the injector in order to avoid the secondary reactions

$$OH + O \rightarrow O_2 + H \quad (2)$$

$$OH + OH \rightarrow H_2O + O \quad (10)$$

This was done because preliminary experiments and computer simulations showed that the increased concentrations of radicals inside the injector could allow formation of relatively large atom concentrations, whereas the much lower concentrations in the main flow tube all but eliminated reactions 2 and 10.

As mentioned in the Introduction, a thorough understanding and characterization of the source chemistry was essential in order to reduce the level of atomic impurities below acceptable limits and allow an accurate determination of k_1. In this work, resonance fluorescence detection of O and H atoms was used to monitor the atomic impurities from a number of source configurations. Source configurations were sought which had oxygen and hydrogen atom densities of 2×10^9 cm^{-3} or less from each source. For a typical initial OH concentration of 10^{11} cm^{-3} this corresponded to $[O]_i + [H]_i \leq 0.04[OH]_i$, and at most a roughtly 6% effect on k_1. It was relatively straightforward to reduce impurities in the HO_2 source by increasing the H_2O_2 concentration and/or the source reaction length in order to react away the impurities via $O + HO_2$ and $H + HO_2$. Unfortunately, this also decreased the HO_2 concentrations, and the decision was made to accept a more limited range of HO_2 concentrations in order to keep the impurity level low. The OH source proved more stubborn initially, until it was determined that the major source of impurity atoms (mainly O) was not from the discharge or secondary chemistry, but rather from the reactions of the F atoms with alumina and exposed glass surfaces of the injector. Teflon coatings on these surfaces proved unsuitable because the high F atom densities caused them to degrade rather quickly. Halocarbon wax coatings are much thicker than the Teflon coatings and proved to hold up better against F atom attack; this allowed reduction of O atoms to below 10^9 cm^{-3}.

Experimental Procedure. Experiments were performed by measuring decays of OH, first in excess H_2O_2, and then in excess HO_2 and H_2O_2. By difference these decays yielded the decay rates of OH due to HO_2 alone. The HO_2 concentrations were measured at the end points of the decay and at one to three points in between; these concentrations were averaged to give the $[HO_2]$ appropriate to the decay. For each experiment, initial concentrations of H_2O_2 and HO_2 were measured, as well as [OH], [O], and [H] from each source separately. Expermental runs with total atoms ([O] + [H]) greater than 4×10^9 cm^{-3} were rejected as unsatisfactory. The initial concentration of fluorine atoms in the HO_2 source was also measured or estimated in order to estimate the concentration of H_2O_2 at the outlet of the source. The decays were corrected for axial diffusion in the usual way;[21] the diffusion coefficient used for OH was 300 cm^2 s^{-1} at 2 Torr.[20]

Data analysis for this reaction was made more complicated by the fact that the reaction of OH with H_2O_2 could neither be ignored nor eliminated. The procedure to measure the decay of OH due to HO_2 alone involved first measuring the OH injector loss and the OH decay due to H_2O_2, combining these to obtain k^-, the first-order decay rate in the absence of HO_2. Then the fluorine discharge was turned on, and the OH decay was measured and combined with injector loss to obtain k^+, the first-order decay rate in the presence of HO_2. Since the H_2O_2 concentration is lowered when the F atoms were added, k^- is an overestimate of the part of k^+ that is not due to HO_2. Therefore, the following procedure for correcting k^- was adopted: the initial concentrations of H_2O_2 and HO_2 were measured, the initial F atom concentration was measured or estimated, and a correction factor was calculated as

$$F_C = \frac{[H_2O_2]_i - [HO_2]_i - \frac{1}{2}([F]_i - [HO_2]_i)}{[H_2O_2]_i} \quad (11)$$

and k_c^- (k^- "corrected") became

$$k_c^- = F_C k^- \quad (12)$$

The expression for F_C was derived from observing that the H_2O_2 concentration coming from the HO_2 source was constrained to be between $[H_2O_2]_i - [HO_2]_i$ and $[H_2O_2]_i - [F]_i$, where the subscript i denotes initial concentration. It was further surmised that all F atoms that were in the probe initially generated HO_2 radicals, but that some of these radicals were lost before emerging due to disproportionation

$$HO_2 + HO_2 \rightarrow H_2O_2 + O_2 \quad (13)$$

Then, $[F]_i = [HO_2]_{probe}$, and $[F]_i - [HO_2]_i$ is the HO_2 which disproportionated in the probe and regenerated H_2O_2. (The probe F atom concentrations were always less than twice the initial HO_2 concentrations, and most typically only about a quarter to a third of the HO_2 produced was lost to disproportionation in the probe before emerging into the tube.) Therefore, via this scheme, $[H_2O]_{tube} = [H_2O_2]_i - [HO_2]_i - \frac{1}{2}([F]_i - [HO_2]_i)$, and eq 11 follows. Finally, the true first-order rate for OH decay due to HO_2 radicals alone was given by

$$k_c^I = k^+ - k_c^- \quad (14)$$

Since the presence of atoms in the reactor in these experiments systematically lowers the observed rate constant below the true rate constant, a simple correction for this effect was attempted. This was done by running computer simulations of each OH decay with and without the O and H atoms, using the initial $[H_2O_2]$, $[HO_2]$, [OH], [O], and [H] measured for each experiment. The difference in the simulated decay rates with and without impurity atoms ranged from about 0.5 to 5 s^{-1}; this correction was added to the measured decay to obtain the final corrected first-order decay rate. The atoms correction amounted to less than 3% for the entire data set. The reactions and rate constants used in the simulations are given in Table I.

Results

The $HO_2 + OH$ reaction was studied by following the decay of OH in excess HO_2 and H_2O_2 for 16 experiments; in addition, the decay of OH in excess H_2O_2 alone was measured in 10 experiments. The experiments were carried out in 2 Torr of helium at 298 K. Table II details the experimental conditions and other information pertinent to this rate constant measurement. Figure

(21) Howard, C. J. *J. Phys. Chem.* **1979**, *83*, 3.

TABLE I: Reactions and Rate Constants Used in Kinetics Simulations

reaction	rate const,[a] cm^3 molecule^{-1} s^{-1}
$OH + HO_2 \rightarrow H_2O + O_2$	8.0×10^{-11}
$OH + OH \rightarrow H_2O + O$	1.9×10^{-12}
$HO_2 + HO_2 \rightarrow H_2O_2 + O_2$	1.7×10^{-12}
$O + OH \rightarrow O_2 + H$	3.1×10^{-11}[b]
$O + HO_2 \rightarrow OH + O_2$	5.2×10^{-11}[b]
$H + HO_2 \rightarrow OH + OH$	6.4×10^{-11}
$H + HO_2 \rightarrow H_2O + O$	3.0×10^{-12}
$H + HO_2 \rightarrow H_2 + O_2$	7.0×10^{-12}
$OH + H_2O_2 \rightarrow HO_2 + H_2O$	1.7×10^{-12}
$O + H_2O_2 \rightarrow OH + HO_2$	1.7×10^{-15}
$H + H_2O_2 \rightarrow OH + H_2O$	1.5×10^{-14}[c]
$H + H_2O_2 \rightarrow HO_2 + H_2$	3.0×10^{-14}[c]
$H + O_2 + He \rightarrow HO_2 + He$	1.1×10^{-15}[d]

[a] From ref 26, except where noted. [b] From ref 20. [c] From ref 27. [d] From ref 28 and 29.

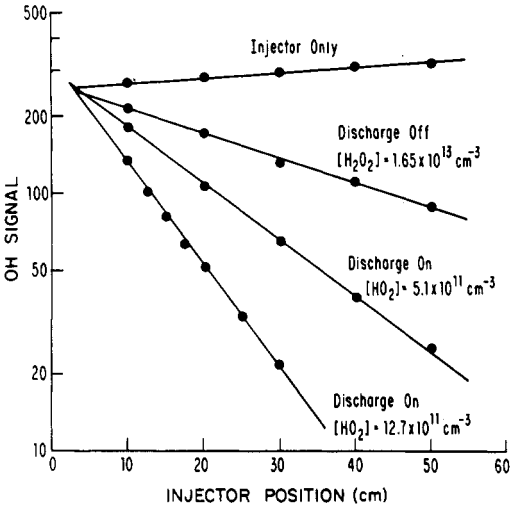

Figure 2. Pseudo-first-order decay plots for the reactions of OH with H_2O_2 and HO_2.

2 shows some measured decays of OH measured with LMR. The top trace shows the injector effect, or probe loss, typically 4–10 s^{-1}. The next trace shows the decay of OH due to H_2O_2 alone, and the bottom decays of OH are due to both HO_2 and H_2O_2. The initial $[H_2O_2]$ was the same for all three decays, and only the initial F atom concentration was varied for the two "discharge on" decays. The first-order decay rate due to HO_2 alone was obtained as explained above by first subtracting some fraction of the "discharge off" decay rate from the discharge on decay rate and then including the small atoms correction.

The 10 experiments which measured OH decays in excess H_2O_2 gave a value of $(2.1 \pm 0.5) \times 10^{-12}$ cm^3 molecule^{-1} s^{-1} for the rate constant for the reaction

$$OH + H_2O_2 \rightarrow HO_2 + H_2O \quad (5)$$

This result is in good agreement with recent measurements.[14,17] For reaction 1, a plot of the first-order decay rate due to HO_2 alone versus the HO_2 concentration is shown in Figure 3. The rate constant from these data has been determined from a least-squares slope–intercept analysis, and by averaging the individual rate constants (which is equivalent to an unweighted least-squares line constrained to pass through the origin). The unweighted least-squares analysis yields a slope of $(7.8 \pm 0.9) \times 10^{-11}$ cm^3 molecule^{-1} s^{-1} and an intercept of -0.7 ± 9.4 s^{-1}. The average of the individual rate constant measurements also gives $(7.8 \pm 1.4) \times 10^{-11}$ cm^3 molecule^{-1} s^{-1}, as expected since the unweighted regression line passes very near the origin. If random errors increase at higher decay rates (and concentrations of HO_2), weights proportional to k_c^I are more appropriate, and the weighted least-squares analysis yields a slope of $(8.2 \pm 1.0) \times 10^{-11}$ cm^3 molecule^{-1} s^{-1} and an intercept of -3.8 ± 12.8 s^{-1}. All reported

TABLE II: OH + HO_2 → H_2O + O_2 Summary[a]

reported rate const, k_1, cm^3 molecule^{-1} s^{-1}	$(8.0\ (+3.0/-2.0)) \times 10^{-11}$ (at $T = 298$ K)
no. of experiments	16
pressure, Torr of He	2.0
flow velocity range, cm s^{-1}	1350–1370
diffusion coeff, cm^2 s^{-1}	OH–He 300 (at 2 Torr)
species detected	HO_2 (LMR) OH (LMR, RF) O (RF) H (RF)
reactant in excess	HO_2
HO_2 concn, cm^{-3}	$(3.1–16.8) \times 10^{11}$
OH initial concn, cm^{-3}	$(7.6–14.0) \times 10^{10}$
initial stoichiometric ratio, $[HO_2]/[OH]_i$	4–18
wall coating	Teflon
first-order wall removal rate, s^{-1}	OH, $k_w^{OH} \leq 5$ HO_2, $k_w^{HO_2} \leq 4$
corrections to obsd first-order decay rates	(1) axial diffusion 0–3% (2) OH probe loss, $k_p = 4–10$ s^{-1}
rate const reported by others, cm^3 molecule^{-1} s^{-1}	(1) $(1.7 \pm 0.5) \times 10^{-11}$ exp[(416 ± 86)/T ($k_{298} = 7.1 \times 10^{-11}$), ref 1c,1b (2) $(4.8 \pm 0.8) \times 10^{-11}$ exp[(250 ± 50)/T] ($k_{298} = 10.8 \times 10^{-11}$), ref 2b (3) $(6.7 \pm 2.3) \times 10^{-11}$ at 295 K, ref 3 (4) $(12 \pm 4) \times 10^{-11}$ at 298 K, ref 4

[a] 1. The rate constant is quite sensitive to the presence of impurity atoms, and special effort was extended to keep their concentrations small. 2. The method used here to determine k_1 required subtracting decay rates with just H_2O_2 present from those with HO_2 and H_2O_2 present.

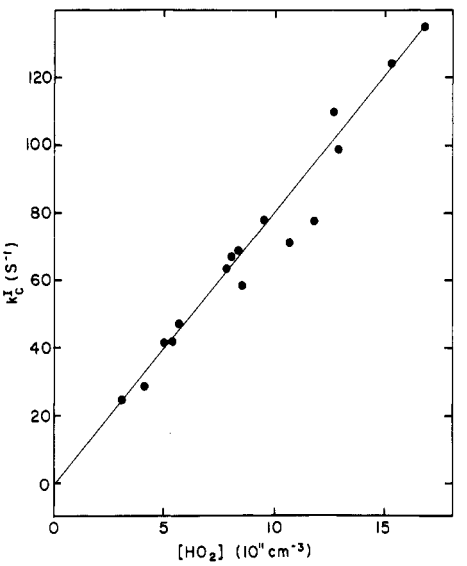

Figure 3. Plot of k_c^I versus $[HO_2]$ for the reaction OH + HO_2 → H_2O + O_2. The line represents a slope of 8×10^{-11} cm^3 molecule^{-1} s^{-1} with zero intercept.

uncertainties are at the 2σ, or 95% confidence level. Including random and possible systematic errors the rate constant for reaction 1 reported here is

$$k_1 = (8.0^{+3.0}_{-2.0}) \times 10^{-11} \text{ cm}^3 \text{ molecule}^{-1} \text{ s}^{-1}$$

The three recent low-pressure, room temperature measurements are in agreement with, but slightly lower than, this value.[1-3] The latest work by Keyser determined in a larger rate constant[2b] and will be discussed further below. It should be noted that any experiment measuring the decay of OH in excess HO_2 yields a lower limit to the true rate constant, since the reactive impurities all tend to regenerate OH, the decaying reactant. Since this has been duly accounted for in the data analysis, it is felt that the above rate constant is accurate to the above limits. It is, however, worth noting that experimental conditions which would allow the measurement of decays of HO_2 in excess OH would in the same way yield an upper limit on the rate constant for this reaction, since the reactive impurities in this case to remove HO_2 above and beyond the removal of HO_2 due to OH alone. A study

measuring the decay of HO_2 in excess OH would be an important confirmation of the recent rate constant measurements for this reaction, all of which measured decays of OH in excess HO_2.

Discussion

It now appears that as a result of the diligent work of many research groups, and in particular Fred Kaufman's group and his former co-worker Leon Keyser, we are closing in on the correct value for k_1. Still, many aspects of the reaction mechanism remain quite controversial and the focus of much debate. The unusual behavior of the OH + HO_2 reaction (i.e., negative temperature dependence, apparent pressure dependence, large rate constant) has led to the common inference that the reaction occurs through a complex-formation mechanism. In this picture the reactants pass through an association transition state to form a relatively long-lived intermediate complex, which subsequently rearranges through a second transition state to form products.[6,22] Yet a combination of experimental evidence (i.e., the coalescence of low- and high-pressure rate constants[2b] and isotope studies[4]) and theoretical work[6,7,22,23] seem to lend increasing support for the dominant role of a hydrogen-atom abstraction mechanism which has a large A factor and slight negative activation barrier due to a hydrogen-bonding type interaction in the entrance channel. (By "hydrogen atom abstraction mechanism" in this paper we mean simply a mechanism whereby the H atom is removed from the HO_2 without a rearrangement from a covalently bonded intermediate.) Both the association–rearrangement and abstracton mechanisms are likely occurring, and the goal of this discussion is to make the case that the abstraction channel is the dominant one.

The recent results from Keyser,[2b] especially combined with the result of this study that the low-pressure value of k_1 appears to be at least 8×10^{-11} cm^3 molecule^{-1} s^{-1}, have called into question the magnitude of the apparent pressure dependence for this reaction. A much smaller or possibly insignificant pressure dependence is indicated by these results, which in turn dictates a more careful consideration of the abstraction mechanism. Indeed, a reaction mechanism with a dominant abstraction mechanism could not support a strong presure dependence within current theoretical frameworks.

It is useful to look at attempts to model the behavior of this reaction within a RRKM framework. In particular, the use of kinetic models with two sequential transition states allows one the flexibility to describe a reaction with a negative temperature dependence and a significant pressure dependence.[6,22] For this system, one brings in the reactants through a loose transition state typical of radical–radical reactions, and proceeds to products through a tight four-center transition state. With this sort of model, one can either match the observed rate constant or the apparent pressure dependence, but not both simultaneously. Briefly stated, in order to obtain a rate constant in reasonable agreement with the measured rate, the height of the second barrier needs to be 8–10 kcal/mol below the energy of the reactants, while in order to obtain a pressure dependence the energy of the second transition state must be close to, or even above that of the first (i.e., the lifetime of the complex must be long enough for it to collisionally stabilize). These studies concluded that the large rate constant is consistent with a fast H-atom abstraction through a loose transition state, but that only a very small pressure-dependent channel could be supported by the experimental data using these models.[6,22] These results make good physical sense, because the four-center rearrangement necessary to pass though the second transition state is highly disfavored due to entropy considerations. Additional evidence that the abstraction channel is dominant comes from a study by Kurylo et al.,[4] who isotopically labeled the hydroxyl radical (^{18}OH) and looked for the formation of $^{18}O^{16}O$ product using a mass spectrometer. They argued that an association–rearrangement mechanism would produce a significant admixture of labeled and unlabeled O_2 product, but they observed only a very small signal from the labeled O_2.

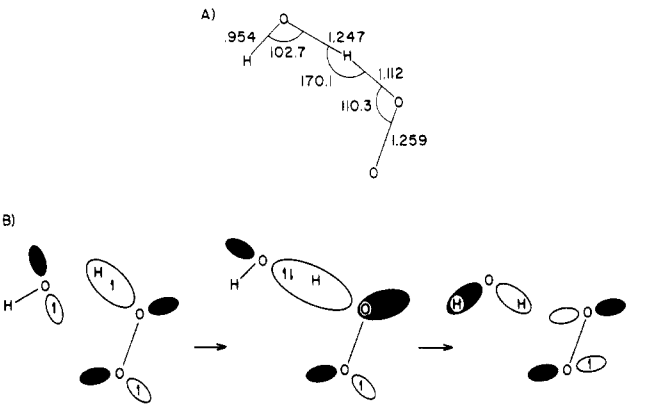

Figure 4. (A) Optimized configuration of the planar transition state for the abstraction channel. Bond lengths are in angstroms and bond angles are in degrees. (B) Frontier orbital diagram of the abstraction reaction.

There is evidence that some HO_2 reactions are predominantely complex and others are predominantly direct. Consider in turn the reactions O + $HO_2 \rightarrow$ OH + O_2 and Br + $HO_2 \rightarrow$ HBr + O_2. A very elegant experiment by Sridharan, Klein, and Kaufman has provided convincing evidence that the O + HO_2 reaction proceeds via a complex mechanism.[16] Their experiment involved isotopically labeling the O atom reactant and monitoring the production of isotopically labeled OH product. They concluded that ^{18}O + HO_2 produces at most a few percent ^{18}OH, that is, direct H-atom abstraction accounts for at most a few percent of the room temperature rate constant, k_3. Therefore, the O atom attacks the O_2 end of the HO_2, and proceeds through a HO_3 intermediate to form $^{18}O^{16}O$ and ^{16}OH products.

On the other hand the reaction of Br + $HO_2 \rightarrow$ HBr + O_2 appears to be consistent with a simple H-atom abstraction mechanism.[7] This is not too surprising, however, for the following reasons. First, the reaction channel to produce OH and BrO products via O–O bond fission is nearly 10 kcal/mol endothermic and is effectively inoperative. Second, the room temperature rate constant is approximately 30 times slower than k_3, and this reaction has a positive temperature dependence. Note that an abstraction channel of this magnitude would be lost in the noise of the addition channel in the O + OH_2 reaction. In fact, a BEBO-type analysis for the Br + HO_2 and OH + HO_2 reactions plotting activation barrier versus exothermicity shows these reactions to be consistent with the theory if one allows that highly exothermic reactions such as OH + HO_2 may have a small negative activation barrier.[7] This small negative activation barrier may be the result of a substantial long-range attraction of the reactants, in this case the result of a hydrogen-bonding type interaction. A recent ab initio calculation on this system found a hydrogen-bonded intermediate to be bound by about 5 kcal/mol,[23] which may explain the negative barrier.

Ab initio calculations have also been carried out in this laboratory in order to identify the dominant frontier orbital interactions and the character of the transition state. The calculations used the 6-31g** basis set of the GAUSSIAN 82 software package.[24] A transition-state optimization for the abstraction channel settled on the planar configuration shown in Figure 4A, and the dominant orbital interaction is that of the singly occupied OH oribtal (predominantly on the O atom) with the H–O bonding 7a′ doubly occupied molecular oribtal of HO_2. This sequence is shown schematically in Figure 4B. The study of Toohey in this issue has explored the potential energy surfaces for abstraction and addition in the X + HO_2 series.[25] Like other reactions in the

(22) Abbatt, J., unpublished work.
(23) Jackels, C. F.; Phillips, D. H. *J. Chem. Phys.* **1986**, *84*, 5013.
(24) Binkley, J. S.; Frisch, M.; Raghavachari, K.; Schlegel, H. B.; Whiteside, R.; Fluder, E.; Seeger, R.; Pople, J. GAUSSIAN 82, Release H; Carnegie-Mellon Univeristy: Pittsburgh, PA.
(25) Toohey, D. W. *J. Phys. Chem.*, this issue.
(26) DeMore, W. B.; Margitan, J. J.; Molina, M. J.; Watson, R. T.; Golden, D. M.; Hampson, R. F.; Kurylo, M. J.; Howard, C. J.; Ravishankara, A. R. "Chemical Kinetics and Photochemical Data for Use in Stratospheric Modeling"; JPL Publication 85-37, NASA, 1985.

series, the OH + HO_2 abstraction channel shows a very early transition state. The calculations also show essentially no barrier to reaction, and the H-bond minimum of ref 23 is also apparent. These calculations are therefore quite consistent with the picture presented so far; that is, the early transition state and a slight minimum in the potential energy surface coupled with essentially no barrier lead to a large cross section for the abstraction channel.

In summary, the "Holy Grail" reaction is still incompletely understood, but a more consistent picture seems to emerge, particularly if one concedes that the pressure dependence is small or negligible. In this picture the dominant mechanism is H-atom abstraction over a loose transition state and the small negative temperature dependence may be explained by an attractive long-range hydrogen-bond interaction between the HO and HOO molecules. The picture is by no means complete, and further study of this fascinating reaction is clearly warranted. Studies which would shed further light on this reaction include: (a) measurement of the products, including the energetically accessible $O_2(^1\Delta)$; (b) additional isotope studies, including $H_2{}^{18}O$ if possible; (c) single studies ranging over large temperature and pressure ranges to observe the onset and falloff of any pressure dependent channels; and (d) studies of decays of HO_2 in excess OH.

Acknowledgment. We acknowledge useful discussions with Darin Toohey and Jon Abbatt. This research was supported the National Science Foundation, Grants ATM-8601126 and CHE-8601431.

Registry No. OH, 3352-57-6; HO_2, 3170-83-0.

(27) Hampson, R. F. "Chemical Kinetic and Photochemical Data Sheets for Atmospheric Reactions"; Report No. FAA-EE-80-17, U.S. Federal Aviation Administration, 1980.
(28) Kurylo, M. J. *J. Phys. Chem.* **1972**, *76*, 3518.
(29) Wong, W.; Davis, D. D. *Int. J. Chem. Kinet.* **1974**, *6*, 401.

Oxygen Atom Exchange in the Interaction of ^{18}OH with Several Small Molecules

Gary D. Greenblatt and Carleton J. Howard*

Aeronomy Laboratory, National Oceanic and Atmospheric Administration, Boulder, Colorado 80303, and Cooperative Institute for Research in Environmental Sciences, University of Colorado, Boulder, Colorado
(Received: March 15, 1988)

Oxygen atom exchange between ^{18}OH and several oxygen-containing molecules was studied in a flow tube by using laser magnetic resonance detection of the reagent ^{18}OH and product ^{16}OH. No significant exchange was observed for O_2, H_2O, CO, CO_2, N_2O, OCS, and SO_2 at 298 and 400 K, and upper limits to the exchange rate coefficients are reported. The rate coefficients for the reactions of ^{18}OH and ^{16}OH with CO were found to be $(1.49 \pm 0.15) \times 10^{-13}$ and $(1.44 \pm 0.15) \times 10^{-13}$ cm^3 $molecule^{-1}$ s^{-1}, respectively, at 298 K. NO and NO_2 were found to exchange rapidly with $k_{ex} = (1.8 \pm 0.6) \times 10^{-11}$ and $(1.0 \pm 0.4) \times 10^{-11}$ cm^3 $molecule^{-1}$ s^{-1}, respectively, at 298 K. On the basis of a simple model of adduct formation k_∞ values for the OH + NO and NO_2 association reactions were estimated to be $\geq(3.6 \pm 1.2) \times 10^{-11}$ and $\geq(1.5 \pm 0.6) \times 10^{-11}$ cm^3 $molecule^{-1}$ s^{-1}, respectively. Error limits are 95% confidence limits.

Introduction

The application of isotopes to kinetics has aided in the analysis of mechanisms,[1] provided information about the geometries of reaction intermediates and potential energy surfaces,[2,3] and has been used to eliminate interference from secondary reactions that regenerate reactants.[4] The effect of quantum mechanical tunneling has been demonstrated by substitution of deuterium for hydrogen atoms.[5] Also the dynamics of reactions that occur through the formation of bound complexes including association reactions and radical-radical reactions can be probed by using isotopically labeled reactants.[6,7]

Oxygen atom exchange has been studied in reactions of isotope-labeled oxygen atoms with NO,[6,8] NO_2,[8] O_2[6,8,9] and HO_2[10] to measure the rate coefficients for the formation of the reaction intermediates. More recently, Van Doren et al.[11] have studied ion-molecule reactions of O^- and have observed rapid isotope exchange between $^{18}O^-$ and CO, SO_2, NO, N_2O, H_2O, CO_2, and O_2. A potentially fertile area of kinetics is the study of oxygen isotope exchange between hydroxyl radicals and oxygen-containing diatomics and triatomics. Hydroxyl radical reactions are fundamental to many combustion processes[12] and to atmospheric chemistry[13] and have been the focus of theoretical studies.[14-17] Examples are the reactions of hydroxyl with nitric oxide and nitrogen dioxide:

$$OH + NO + M \rightarrow HONO + M \quad (1)$$

$$OH + NO_2 + M \rightarrow HONO_2 + M \quad (2)$$

The rate constants for these reactions have been studied by several techniques over a broad range of pressures and temperatures.[18-24]

* Author to whom correspondence should be addressed at NOAA, R/E/AL2, 325 Broadway, Boulder, CO 80303.

(1) Greenblatt, G. D.; Zuckermann, H.; Haas, Y. *Chem. Phys. Lett.* **1987**, *134*, 593.
(2) Gericke, K.-H.; Comes, F. J.; Levine, R. D. *J. Chem. Phys.* **1981**, *74*, 6106.
(3) Butler, J. E.; Jursich, G. M.; Watson, I. A.; Wiesenfeld, J. R. *J. Chem. Phys.* **1986**, *84*, 5365. Cleveland, C. B.; Jursich, G. M.; Trolier, M.; Wiesenfeld, J. R. *J. Chem. Phys.* **1987**, *86*, 3253.
(4) Sinha, A.; Lovejoy, E. R.; Howard, C. J. *J. Chem. Phys.* **1987**, *87*, 2122.
(5) Smith, I. W. M. *Kinetics and Dynamics of Elementary Gas Reactions*; Butterworths: London, 1980; p 195 and references therein.
(6) Anderson, S. M.; Klein, F. S.; Kaufman, F. *J. Chem. Phys.* **1985**, *83*, 1648.
(7) Dransfeld, P.; Lukacs, J.; Wagner, H. Gg. *Z. Naturforsch., A.: Phys., Phys. Chem., Kosmophys.* **1986**, *41*, 1283.
(8) Herron, J. T.; Klein, F. S. *J. Chem. Phys.* **1964**, *40*, 2731.
(9) Brennen, W.; Niki, H. *J. Chem. Phys.* **1965**, *42*, 3725.
(10) Sridharan, U. C.; Klein, F. S.; Kaufman, F. *J. Chem. Phys.* **1985**, *82*, 592.
(11) Van Doren, J. M.; Barlow, S. E.; DePuy, C. H.; Bierbaum, V. M. *J. Am. Chem. Soc.* **1987**, *109*, 4412.
(12) Atkinson, R. *Chem. Rev.* **1986**, *86*, 69.
(13) Graedel, T. E. In *The Photochemistry of Atmospheres*; Levine, J. S., Ed.; Academic: Orlando, FL, 1985.
(14) Smith, I. W. M. *Chem. Phys. Lett.* **1977**, *49*, 112. Smith, I. W. M.; Zellner, R. *J. Chem. Soc., Faraday Trans. 2* **1973**, *69*, 1617.
(15) Zellner, R. *J. Phys. Chem.* **1979**, *83*, 18.
(16) Golden, D. M. *J. Phys. Chem.* **1979**, *83*, 108.
(17) Mozurkewich, M.; Benson, S. W. *J. Phys. Chem.* **1984**, *88*, 6429. Mozurkewich, M.; Lamb, J. L.; Benson, S. W. *J. Phys. Chem.* **1984**, *88*, 6435. Lamb, J. L.; Mozurkewich, M.; Benson, S. W. *J. Phys. Chem.* **1984**, *88*, 6441.
(18) Anderson, J. G.; Margitan, J. J.; Kaufman, F. *J. Chem. Phys.* **1974**, *60*, 3310.

0022-3654/89/2093-1035$01.50/0